Organic & Biomolecular Chemistry

Cite this: *Org. Biomol. Chem.*, 2012, **10**, 8645

www.rsc.org/obc

PAPER

A subnanomolar fluorescent probe for protein kinase CK2 interaction studies†

Erki Enkvist,[a] Kaido Viht,[a] Nils Bischoff,[b] Jürgen Vahter,[a] Siiri Saaver,[a] Gerda Raidaru,[a] Olaf-Georg Issinger,[c] Karsten Niefind[b] and Asko Uri*[a]

Received 25th May 2012, Accepted 4th September 2012
DOI: 10.1039/c2ob26022k

Up-regulation of an acidophilic protein kinase, CK2, has been established in several types of cancer. This cognition has made CK2 an important target for drug development for cancer chemotherapy. The characterization of potential drug candidates, determination of the structure and clarification of the functions of CK2 could be facilitated by the application of small-molecule fluorescent probes that bind to the active site of the enzyme with high affinity and selectivity. We have used a bisubstrate approach for the development of a highly potent inhibitor of CK2. 4,5,6,7-Tetrabromo-1*H*-benzimidazole was conjugated with peptides containing multiple aspartate residues *via* different linkers. The design of the inhibitors was by crystallographic analysis of the complex of an inhibitor with the catalytic subunit of the enzyme (CK2α). The inhibitory potency of the synthesized compounds was established in a kinetic assay that used thin layer chromatography for the measurement of the rate of phosphorylation of fluorescently labelled peptide 5-TAMRA-RADDSDDDDD. The most potent inhibitor, ARC-1502 (K_i = 0.5 nM), revealed high selectivity for CK2α in a panel of 140 protein kinases. Labelling of ARC-1502 with PromoFluor-647 gave the fluorescent probe ARC-1504 that possessed subnanomolar affinity towards both CK2α and the holoenzyme. The probe was used in a fluorescence anisotropy-based binding assay to measure the concentration of CK2α and characterize non-labelled ligands binding to the active site of CK2α.

Introduction

CK2 is a ubiquitous, highly conserved and pleiotropic serine/threonine protein kinase (PK) with numerous physiological functions.[1] It has been estimated that up to 20% of the human phosphoproteome may result from CK2-mediated phosphorylation of its substrate proteins.[2] Activity of CK2 is involved in cell growth, proliferation, angiogenesis, suppression of apoptosis, *etc.*, making the kinase a potential target for cancer chemotherapy.[3] CK2 is constitutively active and does not require pre-phosphorylation or the presence of cofactors for catalytic activity; still, multiple factors modulate its activity allowing specific regulation of cell functions.[1] In cells, CK2 is mostly present in the form of the holoenzyme,[4] a hetero-tetramer composed of two catalytic (α and/or α′) and two regulatory (β) subunits.[5] Both the α-subunit and the holoenzyme are catalytically active but their substrate specificity is different.[6]

CK2 is an acidophilic protein kinase (PK) that prefers substrates containing multiple negatively charged amino acid residues (Asp, Glu or phosphorylated residues) near the phosphoacceptor site,[7] although proteins possessing another kind of amino acid sequences near the phosphorylation site may also be targets of CK2. While numerous crystal structures are available for CK2α subunit,[8] CK2 holoenzyme[5] and complexes of both with various ATP competitive inhibitors,[9,10] the attempts to solve crystal structures of CK2 in complex with peptide substrates have not been successful. Thus the 3D positioning of the residues engaged in binding of a substrate protein has not been established.[11,12]

Several selective ATP-competitive inhibitors of CK2 have been developed in extensive studies. A highly potent and orally available inhibitor, CX-4945, is now in clinical trials for cancer treatment.[10] Non-ATP-competitive inhibitors of CK2 have found less attention[13,14] and only one attempt to design biligand inhibitors that resulted in compounds with micromolar inhibitory potency has been disclosed.[15]

Bisubstrate inhibitors consist of two conjugated fragments, usually structurally related to the substrates (*i.e.*, a phosphoryl

[a]*Institute of Chemistry, University of Tartu, 14A Ravila St., 50411 Tartu, Estonia. E-mail: asko.uri@ut.ee; Tel: +372 7375275*
[b]*Department für Chemie, Institut für Biochemie, Universität zu Köln, Otto-Fischer-Str. 12-14, D-50674 Köln, Germany*
[c]*Institut for Biokemi og Molekylær Biologi, Syddansk Universitet, Campusvej 55, DK-5230 Odense, Denmark*

†Electronic supplementary information (ESI) available: HPLC-MS data of synthesized compounds, selectivity table, X-ray diffraction data and copies of UV, ^{1}H NMR and ^{13}C NMR spectra of new compounds. See DOI: 10.1039/c2ob26022k

group donor and acceptor) of PK.[16] In recent years, the bisubstrate approach to the design of PK inhibitors has made remarkable progress, in some cases leading to inhibitors binding to target kinases with 10 pM K_D-values.[17] Bisubstrate inhibitors well tolerate structural modifications (*e.g.*, insertion of bulky groups or immobilization) without substantial loss of binding affinity. By virtue of this property, they have been used for preparation of high-affinity adsorbents, fluorescent probes and biosensors.[16] Bisubstrate inhibitors incorporating an ATP-competitive fragment and a substrate mimetic might be useful for crystallographic studies for the establishment of the interactions of PK with its protein substrates. Strong interaction of the ATP mimetic facilitates the anchoring of a weakly associating peptide fragment with the kinase thus increasing the possibility for formation of co-crystals where peptide interactions can be solved.[18]

Here we report on the application of a bisubstrate approach to the development of high-affinity ligands for CK2α. The inhibitory potency of the developed ligands was characterized by a thin layer chromatography (TLC)-based kinetic assay that was adapted for the characterization of CK2 inhibitors. The compound with the highest affinity inhibited CK2α-catalysed substrate peptide phosphorylation with a subnanomolar K_i-value. Labelling of the inhibitor with the fluorescent dye PromoFluor-647 gave a high-affinity fluorescent probe that associated with both the free CK2α and the $\alpha_2\beta_2$ holoenzyme. The fluorescent probe was used for determining the concentration of CK2α, measuring the affinities of inhibitors and probing the interaction of CK2α with CK2β.

Results and discussion

Fluorometric TLC-based kinetic assay of CK2 activity

To start the CK2 inhibitor development project, a simple and reliable method was needed for inhibitor characterization. The fluorometric TLC-assay of kinase activity that was previously developed for cAMP-dependent PK (PKA)[19] was now adapted for CK2. The assay is based on the phosphorylation of a fluorescently marked peptide substrate and quantification of both the TLC-separated substrate and its phosphorylation product using fluorescence imaging. For the adaptation of this assay for CK2, a fluorescently labelled peptide, 5-TAMRA-RADDSDDDDD, was synthesized. Thereafter the eluent solution was optimized for good separation of the reaction components. The best results were obtained with a mixture of acetonitrile and ammonia–ammonium acetate buffer at pH 9.5. Since the fluorescence properties of the substrate were not dependent on phosphorylation (data not shown), calculation of the molar ratio of the reaction components was possible on the basis of the signal intensities of the spots without the requirement for calibration. The assay was validated by determination of inhibitory potencies for two previously reported CK2 inhibitors, CX-4945 and K68 (Fig. 1).[20,21] The calculated K_i-values were in good agreement with the values determined previously with a radioactivity-based assay (Table 1). A kinetic CK2 assay based on electrophoretic separation of fluorescently labelled phosphorylated and unphosphorylated peptides has been recently described.[22]

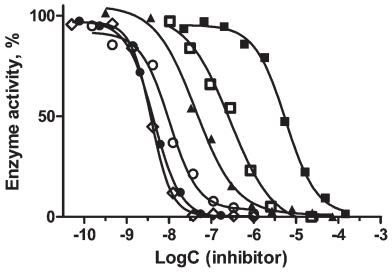

Fig. 1 Inhibition of the activity of CK2α$^{1–335}$ (0.8 nM) with CX-4945 (◊), ARC-1502 in the absence (●) or in the presence (○) of 7.5 μM BSA, ARC-1183 (▲), ARC-1155 (□) and K68 (■) at 30 μM TAMRA-RADDSDDDDD and 100 μM ATP. The calculated IC_{50}-values are summarized in Table 1.

Table 1 Inhibitory potencies and affinities of compounds towards CK2α

Compound	Kinetic assay IC_{50}, nM (pIC_{50}, SE)	FA assay, K_D (SE), nM	+ 10 mM $Mg(OAc)_2$
CX-4945 (K_i = 0.38 nM)[20]	3.8 (8.42, 0.02)	0.56 (0.04)[a]	0.39 (0.04)[a]
ARC-1502	2.7 (8.57, 0.06)	0.52 (0.06)[a]	0.44 (0.04)[a]
ARC-1502 + 7.5 μM BSA	10 (8.99, 0.07)		
ARC-1504	1.8 (8.76, 0.11)	0.39 (0.06)[b]	0.37 (0.07)[b]
ARC-1504 + 100 nM CK2β		0.16 (0.01)[b]	
ARC-1183	30 (7.52, 0.16)	12 (2)[a]	16 (2)[a]
ARC-1154	83 (7.08, 0.19)	22 (3)[a]	22 (3)[a]
ARC-1155	270 (6.56, 0.15)	56 (7)[a]	51 (6)[a]
K68 (K_i = 1.34 μM)[21]	5700 (5.25, 0.05)	1500 (100)[a]	1800 (200)[a]
ATP		>100 000[a]	24 000 (200)[a]
GTP		>100 000[a]	73 000 (2000)[a]

[a] Determined with the FA displacement assay. [b] Determined with the binding assay.

The application of the bisubstrate approach for the working out of potent CK2 inhibitors

We have previously developed high-affinity bisubstrate inhibitors for basophilic PKs of the AGC group.[16] The inhibitors, conjugates of a small ATP-competitive fragment and an arginine-rich peptide (ARC), associated simultaneously with the ATP-binding and protein substrate-binding domains of the target PK. A conjugate could be easily labelled with a fluorescent dye at the side chain amino group of a lysine residue positioned at the C-terminus of the peptide fragment without impairing the binding properties of the conjugate. Here the bisubstrate approach was used for the development of inhibitors of the acidophilic kinase CK2.

A moderately potent and selective CK2 inhibitor, 4,5,6,7-tetrabromo-1*H*-benzimidazole (TBBi), was selected for the role of the ATP-competitive fragment for bisubstrate design and it was conjugated with oligo-aspartate-containing peptides. Firstly, benzimidazole was brominated to 4,5,6,7-tetrabromo-1*H*-benzimidazole[23] and thereafter the product was alkylated with an ester of bromoacetic acid (Scheme 1). Hydrolysis of the ester gave (4,5,6,7-tetrabromo-1*H*-benzimidazol-1-yl)acetic acid (TBBi–acetic acid, K68),[21] which was coupled with the peptides on

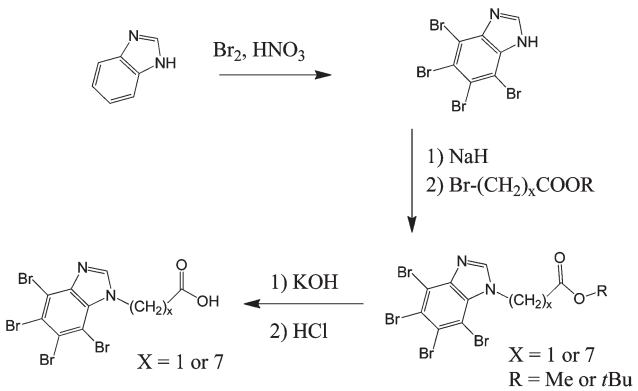

Scheme 1 Synthesis of alkylated TBBi derivatives.

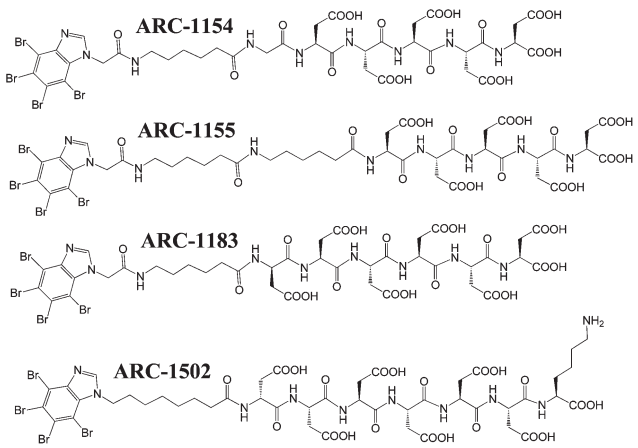

Fig. 2 Structures of ARC-type inhibitors for CK2.

solid phase. Cleavage of the compounds from the resin gave conjugates of TBBi with an oligo-aspartate, compounds ARC-1154 and ARC-1155, differing by the length of the linking fragment (Fig. 2). CK2 inhibition analysis revealed that both compounds possessed sub-micromolar IC_{50}-values, being 20–70-fold more potent than the initial compound, K68 (Table 1).

The structure of the linker may substantially affect the inhibitory potency of a bisubstrate inhibitor. An optimally structured linker enables simultaneous binding of both fragments with low conformational strain and steric repulsion. This may lead to a 3–6 magnitude increase of potency of the conjugate compared to its fragments resulting from the additive binding energies.[16,24] The observed only 70-fold increase in potency showed that the positioning of the fragments was not yet optimal. The structure of the linker in ARC-1154 was thus shortened by excluding the glycine residue. Also a D-aspartic acid molecule was included in the peptide part to test the effect of changing the chirality of the first amino acid in the peptide.[16]

The resulting compound ARC-1183 (Fig. 2) showed a slightly better inhibitory potency (IC_{50} = 30 nM) than ARC-1154 and ARC-1155. For a structural rationalization of this result, ARC-1154 was co-crystallized with $CK2\alpha^{1-335}$ resulting in a crystal structure of medium resolution. The ARC-1154/$CK2\alpha^{1-335}$ co-crystal structure (Fig. 3A) revealed that ARC-1154 occupied – as expected – the ATP-binding site located at the interface between the two main domains; however, only the TBBi–acetic acid moiety of the inhibitor was visible in the electron density while the peptide part was disordered and not defined by electron density.

Comparative structural studies have revealed that the exact orientation of TBBi-related compounds within the ATP-site of CK2α is determined by the origin and positioning of substituents on the five-membered ring.[25] In the case of ARC-1154 the TBBi moiety was turned by more than 60° compared to the positioning of TBBi in the TBBi–acetic acid (K68)/CK2α co-crystal (PDB 3PVG, Fig. 3B).[26] In 3PVG the inhibitor K68 is oriented in such a way that the carboxylate moiety can interact with the Lys68 side chain of CK2α as was found for CX-4945[10] and in all other ATP-competitive CK2α inhibitors containing a carboxylate group.[12] In ARC-1154, however, this orientation is not possible, first, because the carboxylate group of the parent compound K68 is no longer present due to the formation of an amide bond with the linker and second, because the long peptide moiety requires space despite its disorder. As a consequence ARC-1154 is orientated in such a way that the linker/peptide part points towards the substrate binding region of the enzyme (Fig. 3A). The significant higher inhibition potency of ARC-1154 compared to K68 (Table 1) shows that interactions of the peptide moiety with the enzyme indeed occur. Possibly, the disorder in the ARC-1154 region found in the crystal is a consequence of the very high salt concentration (>4 M NaCl) in the crystallization drop that did not favour well-defined ionic interactions between the enzyme and the ligand. Nevertheless, it made sense to check by model building whether a relaxed conformation of ARC-1154 exists in which the peptide region is in direct contact to the enzyme's positively charged determinants of substrate recognition. Since no experimental structure of CK2α or the CK2 holoenzyme with a peptide substrate has been disclosed, we took the model of human CK2α in complex with the peptide DSDDD as a guideline.[27] This model had been created on the basis of the crystal structure of CK2α with two sulphate ions (PDB 2PVR) that mark the binding sites for the negatively charged side chains of P + 1 and P + 3 amino acid residues of a CK2 substrate. Accordingly, the conformations of the linker and the peptide region of ARC-1154 were changed in a plausible way to afford a close contact of the penta-aspartate moiety with the interacting amino acid residues of the substrate binding site of CK2α (Fig. 3C).

In the next stage of the structure optimization, the rigid amide group was removed to increase the flexibility of the linker. Octanoic acid was used to retain a comparable length of the linker to that in ARC-1183. TBBi was alkylated with 8-bromooctanoic acid methyl ester in the presence of NaH (Scheme 1). After hydrolysis of the methyl ester, the yielded 8-(4,5,6,7-tetrabromo-1*H*-benzimidazol-1-yl)octanoic acid (TBBi–octanoic acid) was coupled to the peptide. A lysine residue was added to the C-terminus of the conjugate as a possible site for the attachment of fluorescent labels. The resulting compound ARC-1502 (Fig. 2) incorporated a TBBi moiety, an octanoic acid linker, an oligo-aspartate peptide, and a lysine residue. The inhibitory potency of ARC-1502 (IC_{50} = 2.7 nM, Fig. 1) was about 10-fold higher than the inhibitory potency of ARC-1183. The calculated K_i-value of 0.5 nM is very close to the K_i-value of CX-4945[20] and about 1000-fold smaller than that of TBBi,[21,23] indicating that in the case of a flexible linker both fragments of the conjugate TBBi and oligoaspartate can simultaneously interact with CK2α resulting in subnanomolar inhibitory potency of the compound.

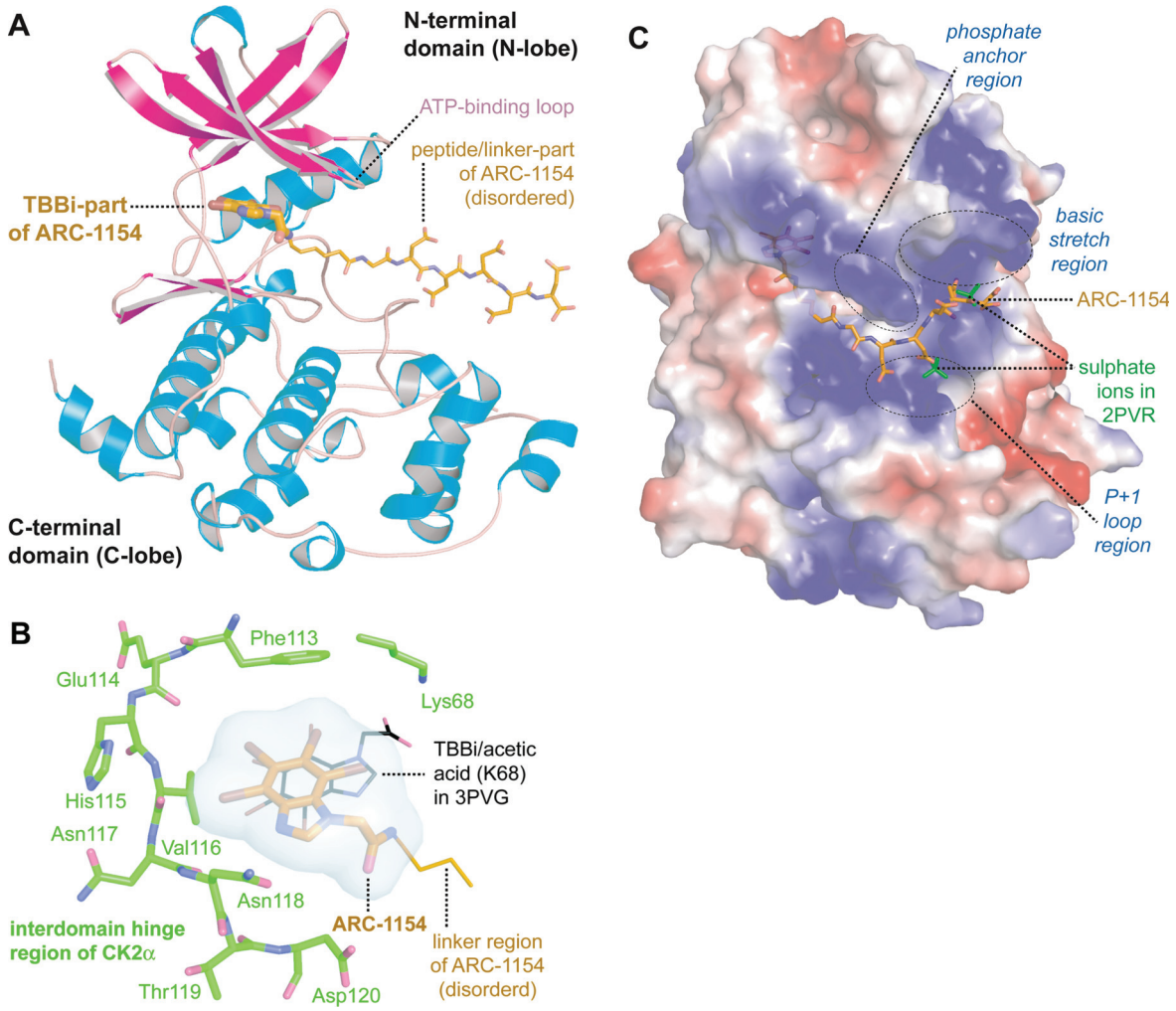

Fig. 3 The bisubstrate inhibitor ARC-1154 occupies the ATP-binding site of CK2α$^{1–335}$. (**A**) Overview of the CK2α$^{1–335}$/ARC-1154 complex structure (PDB 4FBX). Only the TBBi-moiety plus the peptide group forming the connection to the linker/peptide region is defined by electron density. The highly charged peptide region and the linker are disordered; they are included in the figure for illustration and are shown in a standard conformation. (**B**) Magnified view of the ATP-site occupied by the TBBi-moiety of ARC-1154. For comparison, the K68 inhibitor (TBBi–acetic acid), as found in PDB file 3PVG, is drawn (black sticks) after superimposition of the protein matrices. The ordered and visible part of the ARC-1154 inhibitor is covered by a transparent surface for illustrative reasons. (**C**) Electrostatic surface representation (blue: positive charge; red: negative charge) with the penta-aspartate section for ARC-1154 modelled to the substrate binding and recognition site. Three positively charged regions important for the recognition of acidic substrate proteins are indicated by ellipses. Two sulphate ions as found in PDB structure 2PVR are drawn in green colour; they indicate the binding sites for the acidic P + 1 and P + 3 side chains, the most important determinants within the canonical recognition sequence of CK2 substrates. All parts of the figure were drawn with PyMOL (Schrödinger Ltd).

The inhibition selectivity of ARC-1502 was tested with 140 PKs (Table 2). Only ten kinases in this panel were inhibited by more than 50% with 1 μM ARC-1502. These kinases mostly belong to the CMGC group of PKs. ARC-1502 showed remarkable selectivity towards CK2 for which the strongest inhibition was observed (1% residual activity at 1 μM concentration of ARC-1502), followed by more than 10-fold weaker inhibition (if calculated into IC_{50} scale) of DYRK2 and PLK1. The obtained selectivity profile for ARC-1502 is different from that of the parent compound TBBi. The latter compound, like many other ATP-competitive CK2 inhibitors, comparably or better inhibits PKD1 and kinases of the DYRK and PIM families.[26,29] ARC-1502 has good potency to inhibit acidophilic kinases CK2 and PLK1 while basophilic kinases of the PIM family, Aurora B, ROCK2 and smMLCK are much less inhibited. The increased selectivity of ARC-1502 towards acidophilic protein kinases can be attributed to the presence of the oligoaspartate moiety in the structure of the inhibitor. Based on the data, a Gini coefficient of 0.616 was calculated[30] for ARC-1502 which is close to that obtained for selective inhibitors of the CX-series.[29] The results demonstrate that by the conjugation of a peptide fragment and an ATP-pocket-targeted moiety it is possible to develop bisubstrate inhibitors for CK2 that have substantially higher selectivity and potency than the parent compounds.

Binding assay with fluorescence anisotropy/polarization readout

Inhibitors labelled with fluorescent dyes have great value in biochemical, biological and medicinal research. These inhibitors

Table 2 Residual activities of PKs[a] in the presence of ARC-1502 (1 μM) and TBBi (10 μM, published selectivity profile)

		Residual activity (%)	
PK	Kinase group	ARC-1502, 1 μM	TBBi, 10 μM[28]
CK2	Other	1 (±0)	10
DYRK2	CMGC	17 (±1)	9
PLK1	Other	18 (±3)	29
CLK2	CMGC	24 (±2)	
ERK8	CMGC	25 (±0)	11
DYRK3	CMGC	30 (±2)	6
DYRK1A	CMGC	36 (±3)	3
HIPK2	CMGC	36 (±1)	3
GSK3β	CMGC	46 (±7)	41
CK1δ	CK1	49 (±5)	
PIM3	CAMK	59 (±3)	2
PIM1	CAMK	62 (±10)	2
PKD1	CAMK	72 (±7)	5
HIPK3	CMGC	75 (±0)	9
ROCK2	AGC	91 (±5)	31
PIM2	CAMK	92 (±0)	2
smMLCK	CAMK	96 (±1)	11
PKA	AGC	100 (±2)	75
Aurora B	Other	100 (±19)	15

[a] Residual activities are expressed as a percentage of the control without an inhibitor (by means of duplicate determinations). Complete table with 140 kinases is included in the ESI.†

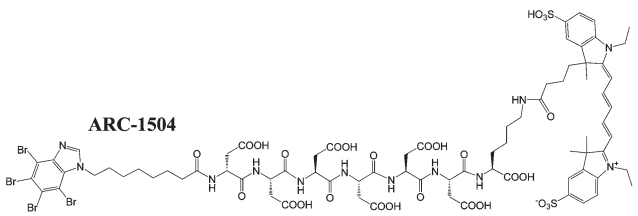

Fig. 4 Structure of the fluorescent ligand ARC-1504.

can be used as fluorescent probes for monitoring of enzyme activity and localization in a variety of assays from inhibitor screening to cell, tissue and live organism imaging. Small-molecule high-affinity fluorescent probes have been described for several PKs,[31,32] but to the best of our knowledge such probes have not been disclosed for CK2. The inhibitor ARC-1502 was labelled with the dye PromoFluor-647 to yield the fluorescent probe ARC-1504 (Fig. 4). The probe was characterized in an assay with fluorescence anisotropy (FA) readout. A fixed concentration of ARC-1504 was titrated with a concentration series of CK2α on a 384-well microtitre plate in 20 μL volumes. The fluorescence anisotropy value of the solutions was measured at 590 nm excitation and 675 nm emission wavelengths (Fig. 5). The titration was first performed in a BSA-containing buffer. A nearly constant signal was registered over the full range of applied concentrations of CK2α indicating a possible interaction between BSA and ARC-1504. Titration of the fluorescent probe with BSA showed a concentration-dependent increase of anisotropy that became saturated at concentrations of the protein above 10 μM (data not shown), revealing that ARC-1504 was indeed associated with BSA at the concentration (7.5 μM) used in the first titration experiment. The presence of BSA also increased the IC_{50}-value for ARC-1502 in the kinetic assay (Fig. 1). After excluding BSA from the FA-assay buffer, titration of ARC-1504 with CK2α could be performed, leading to an increase of about 10% in the fluorescence intensity and of about 150 milliunits in the anisotropy values compared to the signals from the free probe. The titration at low concentrations of the fluorescent probe (C = 0.2 nM) yielded a K_D-value of 0.4 nM for the ARC-1504/CK2α interaction. The binding constants coincided in the presence and in the absence of magnesium ions in solution. From the titration curve measured at a much higher concentration of the fluorescent ligand ARC-1504 than the K_D-value (in tight-binding conditions), the concentration of the active form of the enzyme was calculated.[33] The content of the active kinase in the used enzyme stock solution was typically between 20–60% of the total protein and the calculated amount of the active kinase in the sample correlated well with the catalytic activity of the enzyme.

Next, in a FA-based assay, displacement of the fluorescent probe ARC-1504 from the complex with CK2α was performed with commercially available ATP-competitive inhibitors CX-4945 and K68, and compounds developed in this study. Displacement of ARC-1504 by ATP and GTP was also tested since CK2 can use both nucleotides as co-substrates in the phosphorylation reaction.[34] ARC-1504 was at least partly displaced by all tested compounds (Fig. 6). Values of the displacement constants

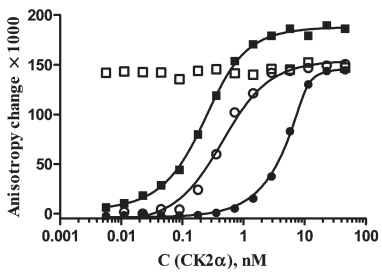

Fig. 5 Titration of 10 nM ARC-1504 (●) or 0.2 nM ARC-1504 (○,■,□) with CK2α$^{1–335}$ in the presence of 100 nM CK2β (■) or 7.5 μM BSA (□). The concentration of CK2α$^{1–335}$ in the x-axis corresponds to the active form of the enzyme. Anisotropy changes are given relative to the free ligand (10 nM). The calculated binding constants are summarized in Table 1.

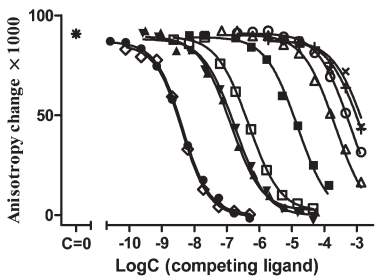

Fig. 6 Displacement of ARC-1504 (3 nM) from the complex with CK2α$^{1–335}$ (2 nM) with CX-4945 (◊), ARC-1502 (●), ARC-1183 (▲), ARC-1154 (▼), ARC-1155 (□), K68 (■), ATP (Δ) and GTP (○), all in the presence of 10 mM $Mg(OAc)_2$, and ATP (×) and GTP (+) in the absence of $Mg(OAc)_2$. Anisotropy changes are given relative to the free ligand (3 nM). The calculated displacement constants are summarized in Table 1.

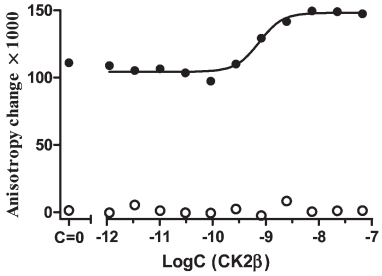

Fig. 7 Titration of ARC-1504 (0.5 nM) with CK2β in the presence (●) and in the absence (○) of $CK2\alpha^{1-335}$ (0.8 nM). Anisotropy changes are given relative to the free ligand (5 nM). Fitting the data to a sigmoidal dose–response model gave an EC_{50}-value of 0.8 nM.

(K_d) calculated for the compounds correlated well with their inhibitory potencies determined in the kinetic assay in this work as well as with potencies reported in literature (Table 1). As expected, the binding of ATP and GTP was tighter in the presence of magnesium ions, while other competing ligands did not show such dependency.

It was further investigated how ARC-1504 was binding to the CK2 holoenzyme. The association of CK2α with ARC-1504 in the presence of an excess of CK2β occurred with about 2.5-fold higher affinity than with the free catalytic subunit (Fig. 5). The higher affinity for the holoenzyme is consistent with the fact that CK2β increases the catalytic activity of CK2α for peptide substrates.[35] The complex ARC-1504/$CK2\alpha_2\beta_2$ showed 20% higher anisotropy value (185 milliunits) than the complex with the free catalytic subunit while no anisotropy change was detected in the presence of free CK2β (Fig. 5 and 7). The anisotropy difference between these complexes can be attributed to the more than 3-fold higher molecular mass of the holoenzyme compared to the free α-subunit (135 *vs.* 40 kDa). These results demonstrate that ARC-1502-based fluorescent probes can be used for the investigation of the interactions of the catalytic subunit of CK2α with its regulatory subunit CK2β or other proteins.

Conclusions

A bisubstrate inhibitor approach was efficiently used for CK2. 4,5,6,7-Tetrabromo-1*H*-benzimidazole was coupled with oligo-aspartic acid-containing peptides through different linkers. The conjugate ARC-1502 containing a flexible octanoic acid linker is a highly selective tight-binding inhibitor of CK2α with subnanomolar inhibitory potency (K_i = 0.5 nM). Labelling of ARC-1502 with PromoFluor-647 gave a fluorescent probe, ARC-1504, possessing subnanomolar affinity (K_d = 0.4 nM) for CK2α. Fluorescent probes with such high affinity have not been described for CK2 previously. ARC-1504 can be used in a FA-based assay to measure the concentration of active CK2 and to characterize non-labelled inhibitors in displacement experiments. Titration of the ARC-1504/CK2α complex with CK2β led to an increase of the FA value pointing to the possibility of using ARC-1504 as a fluorescent probe to study interactions of CK2α with other proteins.

Fluorescence-based activity assays are safer and more user friendly than radiometric assays. The developed kinetic assay based on TLC separation of fluorescent reaction components is a simple alternative to radiometric assays. A good correlation between inhibitory potencies and binding affinities was obtained for all tested compounds.

The solved ARC-1154/CK2α co-crystal structure indicated that the novel biligand compounds could be used for crystallographic studies. This achievement gives hope that co-crystals of ARC-1502 with the free catalytic subunit and holoenzyme of CK2 will be obtained in the future that shed light upon interactions in the CK2 substrate site beyond the level of theoretical modelling. To achieve this goal crystallization conditions with significantly lower salt concentration could be beneficial.

Experimental

Materials and equipment

Chemicals were obtained from the following commercial sources: NovaBiochem and Iris Biotech GmbH (peptide synthesis reagents), Scharlau (TFA), Alfa Aesar (triisopropylsilane), PromoKine (PromoFluor-647 NHS ester), Anaspec (5-TAMRA NHS ester), Deutero GmbH (deuterated solvents) and Synkinase (CX-4945). Other chemicals and solvents were obtained from Sigma-Aldrich, Scharlau, Riedel-de Haën and Fluka. TLC plates were obtained from Macherey-Nagel. Biochemical assays were carried out on black low-volume 384-well nonbonding-surface polystyrene microplates (Corning cat. no. 3676).

C-terminal deletion mutant $CK2\alpha^{1-335}$ was used because of its higher stability compared to the wild-type protein. $CK2\alpha^{1-335}$ was prepared as described previously.[36] The concentration of $CK2\alpha^{1-335}$ was determined in the FA-assay as described below.

The concentrations of the ligands were determined spectrophotometrically on a NanoDrop 2000c spectrophotometer (Thermo Scientific) in a buffer (50 mM HEPES, pH = 7.5) using molar extinction coefficients of 15 000 M^{-1} cm^{-1} (260 nm) for ATP, 13 700 (253 nm) M^{-1} cm^{-1} for GTP, 9000 M^{-1} cm^{-1} (360 nm) for CX-4945, 10 000 M^{-1} cm^{-1} (265 nm) for TBBi-containing compounds, 250 000 M^{-1} cm^{-1} (650 nm) for PromoFluor-647-labeled compounds and 80 000 (552 nm) M^{-1} cm^{-1} for 5-TAMRA-labeled compounds.

The purification of the compounds was performed on a Shimadzu Prominence LC Solution HPLC system with a SPD M20A diode array detector and a Phenomenex Gemini C18 5 µm column (250 × 4.6 mm) protected by a 5 µm Gemini C18 (4 × 2.0 mm) guard column at a flow rate of 1 ml min^{-1}. Mass spectra were measured in positive ion mode on Thermo Electron LTQ Orbitrap (ESI HRMS) and Schimadzu LCMS-2020 (ESI-MS). Monoisotopic masses are presented in the case of HRMS data. ^1H and ^{13}C NMR spectra were recorded on a Bruker AC 200P NMR spectrometer. Fluorescence spectra were measured on Fluoromax-4 (Horiba). Fluorescence anisotropy was measured on a PHERAstar platereader (BMG Labtech) with a FA optical module [ex 590 (50) nm, em 675 (50) nm]. Fluorescence imaging was performed on a Molecular Imager FX (Bio-Rad) at 532 nm excitation wavelength (diode-pumped solid-state laser) and 555 nm LP emission filter, 100 µm per pixel. Scanned images were processed by Quantity One software (version 4.6.6, Bio-Rad). Graphpad Prism software (version 5.04, GraphPad) was used for data analysis.

Synthesis

The synthesis and characterization of 4,5,6,7-tetrabromo-1*H*-benzimidazole[23] and (4,5,6,7-tetrabromo-1*H*-benzimidazol-1-yl)-acetic acid have been previously described.[21] Alkylation of 4,5,6,7-tetrabromo-1*H*-benzimidazole was slightly modified by using NaH as the base and DMF as the solvent.

8-(4,5,6,7-Tetrabromo-1*H*-benzimidazol-1-yl)octanoic acid. 4,5,6,7-Tetrabromo-1*H*-benzimidazole (115 mg, 0.26 mmol) and NaH suspension (12 mg, ~0.28 mmol) were stirred in DMF for 30 min, then 8-bromooctanoic acid methyl ester (182 mg, 0.77 mmol) was added. The solution was stirred for 2 days and then evaporated to dryness. The residue was purified by flash chromatography ($CHCl_3$: methanol; 20 : 1). The methyl ester was hydrolyzed in the mixture of methanol and aqueous KOH. After 1 h the solvents were removed *in vacuo* and the residue was partitioned between ethyl acetate and $KHSO_4$, the organic layer was dried and evaporated to yield 8-(4,5,6,7-tetrabromo-1*H*-benzimidazol-1-yl)octanoic acid (95 mg, 62% over two steps). HRMS *m*/*z* calcd for $C_{15}H_{16}Br_4N_2O_2$ $[M + H]^+$: 572.80180, found: 572.80062.

δ_H (200 MHz; $DMSO_{6d}$; Me_4Si) 1.28 (m, 6H), 1.48 (m, 2H), 1.79 (m, 2H), 2.19 (t, J = 7.3 Hz, 2H), 4.48 (t, J = 7.6 Hz, 2H), 8.51 (s, 1H), 11.96 (br, 1H).

δ_C (50 MHz; $DMSO_{6d}$; Me_4Si) 24.3, 25.5, 28.1, 28.3, 31.4, 33.5, 46.4, 106.5, 116.5, 120.3, 122.3, 131.2, 143.6, 148.7, 174.3.

Synthesis of peptide conjugates

Peptide fragments were prepared by using traditional Fmoc solid-phase peptide synthesis methods on the Wang resin. Protected amino acids (3 eq) were dissolved in DMF and activated with HBTU/HOBt (2.94 eq each) and *N*-methylmorpholine (9 eq) in DMF. After 3 min, the coupling solutions were added to the resin (about 1 ml/100 mg of resin) and shaken for 40–60 min at rt. The completeness of each step was monitored with the Kaiser-test. Removal of the Fmoc-group was performed with 20% piperidine solution in DMF (20 min). Fmoc-protected linkers were attached to the peptide part following the same protocol. The coupling of (4,5,6,7-tetrabromo-1*H*-benzimidazol-1-yl)acetic acid and 8-(4,5,6,7-tetrabromo-1*H*-benzimidazol-1-yl)-octanoic acid to the peptides was carried out with 1.5 eq of the appropriate acid activated with HOBt/HBTU (1.47 eq each) in DMF/*N*-methylmorpholine and added to the resin and shaken for at least 3 h. Finally the resins were washed 5 times with each solvent (DMF, isopropanol, DCE) and dried. Treatment with TFA–H_2O–triisopropylsilane (90 : 0.5 : 5 by volume) for 2–3 h was used as the standard cleavage procedure releasing the conjugate as C-terminal carboxylic acid. The products were purified by reversed phase HPLC with ACN/0.1% TFA gradient and lyophilized.

ARC-1154 HRMS *m*/*z* calcd for $C_{37}H_{43}Br_4N_9O_{19}$ $[M + H]^+$: 1233.94815, found: 1233.94278.

ARC-1155 HRMS *m*/*z* calcd for $C_{41}H_{51}Br_4N_9O_{19}$ $[M + H]^+$ 1290.01075, found 1290.01108.

ARC-1183 HRMS *m*/*z* calcd for $C_{39}H_{45}Br_4N_9O_{21}$ $[M + H]^+$ 1291.95363, found 1291.95327.

ARC-1502 HRMS *m*/*z* calcd for $C_{45}H_{58}Br_4N_{10}O_{21}$ $[M + 2H]^{+2}$ 696.03285, found 696.03265, $[M + H]^+$ 1391.05843, found 1391.05635.

ARC-1504. ARC-1502 was labelled with PromoFluor-647 at the side-chain of the lysine residue in a mixture of NHS-activated fluorescence label (1.2 eq), TEA (10–50 eq) in DMF, 3 h at rt. The solvent was removed *in vacuo*, the product was purified by HPLC with ACN–0.1% TFA gradient and lyophilized. ESI HRMS *m*/*z* calcd for $[M + 2H]^{+2}$ 1008.13160, found 1008.13173.

5-TAMRA-Arg-Ala-$(Asp)_2$-Ser-$(Asp)_5$. 5-TAMRA was introduced to the N-terminus of the purified peptide in a mixture of NHS-activated fluorescence label (1.1 eq) and DIPEA (~50 eq) in DMSO, 5 h at rt. The product was precipitated by the addition of 10 times excess volume of methyl *tert*-butyl ether, centrifuged, purified by HPLC with ACN–0.1% TFA gradient and lyophilized. HRMS *m*/*z* calcd for $C_{65}H_{80}N_{15}O_{30}$ $[M + 2H]^{+2}$: 775.76314, found: 775.76188; fluorescence (50 mM Hepes, pH 7.5, 150 mM NaCl, 0.005% tween 20) ex λ_{max}: 552 nm, em λ_{max}: 579 nm.

FA-based binding/displacement assay

The assay was carried out in a buffer containing: HEPES (50 mM, pH 7.5), NaCl (150 mM), DTT (5 mM), EDTA (0.1 mM) and tween 20 (0.005%) in 20 μL volumes. The concentration of the active kinase was determined in a binding assay by titration of ARC-1504 (10 nM) with CK2α (2-fold dilutions). Binding constants were determined in the same way at a smaller concentration of ARC-1504 (0.2 nM). The displacement assay was performed at constant concentration of $CK2\alpha^{1–335}$ (2 nM) and ARC-1504 (3 nM) using 3-fold dilutions of the competitors. The microplates were incubated for 15 min at 30 °C before measurement. The obtained data were analyzed and binding and displacement constants were calculated as described previously.[33]

Phosphorylation assay

The inhibitory potencies were measured in mixtures containing: the inhibitors (3-fold dilutions), the kinase (0.8 nM), ATP (100 μM), the peptide substrate 5-TAMRA-RADDSDDDDD (30 μM), $Mg(OAc)_2$ (10 mM), and other buffer components as for the FA assay. The solution was incubated for 10 min at the assay temperature (30 °C) before the phosphorylation was initiated by the addition of the peptide substrate. At fixed time points, the reaction was terminated by a 20-fold dilution of an aliquot from the incubation medium with aqueous trifluoroacetic acid (1%). The solutions were analyzed by TLC on normal-phase silica gel plates without fluorescent indicator using the eluent system of 20% acetonitrile–1.7 M ammonium acetate–1.3 M ammonium hydroxide (pH = 9.5). After drying the plate was visualized by fluorescence imaging. The concentration of the phosphorylated peptide in the reaction mixture was calculated from the ratio of the integrated intensity of the spot corresponding to the phosphopeptide to the sum of intensities of the spots corresponding to the phosphopeptide and unreacted substrate. The obtained inhibition data was fitted to a sigmoidal dose–response model. The K_i-values were calculated for tight-binding competitive inhibitors as described previously.[37] A small amount

of phosphorylated product was purified from the phosphorylation mixture by HPLC with ACN–0.1% formic acid gradient, lyophilized and characterized. HRMS *m/z* calcd for $C_{65}H_{81}N_{15}O_{33}P$ $[M + 2H]^{+2}$: 815.74631, found: 815.74562, fluorescence (50 mM Hepes, pH 7.5, 150 mM NaCl, 0.005% tween 20) ex λ_{max}: 551 nm, em λ_{max}: 578 nm.

Crystallization and X-ray structure determination

The concentrated CK2α$^{1-335}$ solution contained 6.2 mg ml^{-1} protein dissolved in 500 mM NaCl, 25 mM Tris HCl, pH 8.5. Nine volume parts of this protein stock solution were mixed with one part 12 mM ARC-1154 dissolved in 100% dimethyl sulfoxide. The CK2α$^{1-335}$/ARC-1154 mixture was incubated for 30 min at room temperature and afterwards used for crystallization experiments by sitting drop vapour diffusion. The best crystals grew with a reservoir solution composed of 4.4 M NaCl, 100 mM citric acid, pH 5.25 and mixing 2 µl of this reservoir solution with 4 µl CK2α$^{1-335}$/ARC-1154 mixture. For X-ray diffractometry the CK2α$^{1-335}$/ARC-1154 crystals were mounted directly from the crystallization drops, *i.e.*, without application of a special cryo protocol. An X-ray diffraction data set was collected at 100 K with a SuperNova-diffractometer from Agilent Technologies. The data were indexed and integrated with XDS[38] and scaled with SCALA from the CCP4 program suite.[39] For structure solution by molecular replacement and subsequent refinement the corresponding modules of PHENIX[40] were used. Manual corrections were performed with COOT.[41] The final atomic coordinates together with the experimental structure factors were deposited at the Protein Data Base (www.rcsb.org; accession code 4FBX).

Theoretical modelling

For the construction of the CK2α$^{1-335}$/ARC-1154 model illustrated in Fig. 3C we used COOT[41] to delete interfering water molecules in the substrate binding region and to change the conformation of the linker and the peptide part of ARC-1154 in such a way that the aspartate side chains came into contact with the positively charged zones substrate recognition regions of the enzyme. A rough model created manually was optimized by PHENIX[40] refinement run including a molecular dynamics calculation following a simulated annealing protocol.

Kinase selectivity panel

The selectivity profiling of ARC-1502 was performed in a panel with 140 PKs using radiometric filter-binding assay (on commercial basis by International Centre for Kinase Profiling, University of Dundee). The final concentration of the inhibitor in the assay was 1 µM and the concentration of ATP was at or below the calculated K_m value for the kinase or above K_m value for some kinases (MKK6, MPSK1, STK33 and ASK1).

Acknowledgements

The work was supported by grants from the Estonian Science Foundation (8230, 8419 and 8055), the Estonian Ministry of Education and Sciences (SF0180121s08), the Deutsche Forschungsgemeinschaft (NI 643/4-1), the Danish Cancer Society (OGI 252-1109-210) and the Danish Research Council (21-04-0517).

Notes and references

1 M. Montenarh, *Cell Tissue Res.*, 2010, **342**, 139–146.
2 M. Salvi, S. Sarno, L. Cesaro, H. Nakamura and L. A. Pinna, *Biochim. Biophys. Acta*, 2009, **1793**, 847–859.
3 J. H. Trembley, G. Wang, G. Unger, J. Slaton and K. Ahmed, *Cell. Mol. Life Sci.*, 2009, **66**, 1858–1867.
4 M. Salvi, S. Sarno, O. Marin, F. Meggio, E. Itarte and L. A. Pinna, *FEBS Lett.*, 2006, **580**, 3948–3952.
5 K. Niefind, B. Guerra, I. Ermakowa and O. G. Issinger, *EMBO J.*, 2001, **20**, 5320–5331.
6 F. Meggio, B. Boldyreff, O. Marin, L. A. Pinna and O. G. Issinger, *Eur. J. Biochem.*, 1992, **204**, 293–297.
7 L. A. Pinna and M. Ruzzene, *Biochim. Biophys. Acta.*, 1996, **1314**, 191–225.
8 K. Niefind, B. Guerra, L. A. Pinna, O. G. Issinger and D. Schomburg, *EMBO J.*, 1998, **17**, 2451–2462.
9 R. Battistutta, M. Mazzorana, L. Cendron, A. Bortolato, S. Sarno, Z. Kazimierczuk, G. Zanotti, S. Moro and L. A. Pinna, *ChemBioChem*, 2007, **8**, 1804–1809.
10 F. Pierre, P. C. Chua, S. E. O'Brien, A. Siddiqui-Jain, P. Bourbon, M. Haddach, J. Michaux, J. Nagasawa, M. K. Schwaebe, E. Stefan, A. Vialettes, J. P. Whitten, T. K. Chen, L. Darjania, R. Stansfield, K. Anderes, J. Bliesath, D. Drygin, C. Ho, M. Omori, C. Proffitt, N. Streiner, K. Trent, W. G. Rice and D. M. Ryckman, *J. Med. Chem.*, 2011, **54**, 635–654.
11 K. Niefind, J. Raaf and O. G. Issinger, *Cell. Mol. Life Sci.*, 2009, **66**, 1800–1816.
12 R. Battistutta, *Cell. Mol. Life Sci.*, 2009, **66**, 1868–1889.
13 B. Laudet, C. Barette, V. Dulery, O. Renaudet, P. Dumy, A. Metz, R. Prudent, A. Deshiere, O. Dideberg, O. Filhol and C. Cochet, *Biochem. J.*, 2007, **408**, 363–373.
14 V. Moucadel, R. Prudent, C. F. Sautel, F. Teillet, C. Barette, L. Lafanechere, V. Receveur-Brechot and C. Cochet, *Oncotarget*, 2011, **2**, 997–1010.
15 R. Świder, M. Masłyk, S. Martín-Santamaría, A. Ramos and B. de Pascual-Teresa, *Mol. Cell. Biochem.*, 2011, **356**, 117–119.
16 D. Lavogina, E. Enkvist and A. Uri, *ChemMedChem*, 2010, **5**, 23–34.
17 M. Kasari, P. Padrik, A. Vaasa, K. Saar, K. Leppik, J. Soplepmann and A. Uri, *Anal. Biochem.*, 2012, **422**, 79–88.
18 A. Pflug, J. Rogozina, D. Lavogina, E. Enkvist, A. Uri, R. A. Engh and D. Bossemeyer, *J. Mol. Biol.*, 2010, **403**, 66–77.
19 K. Viht, A. Vaasa, G. Raidaru, E. Enkvist and A. Uri, *Anal. Biochem.*, 2005, **340**, 165–170.
20 A. Siddiqui-Jain, D. Drygin, N. Streiner, P. Chua, F. Pierre, S. E. O'Brien, J. Bliesath, M. Omori, N. Huser, C. Ho, C. Proffitt, M. Schwaebe, D. M. Ryckman, W. G. Rice and K. Anderes, *Cancer Res.*, 2010, **70**(24), 10288–10298.
21 A. Gianoncelli, G. Cozza, A. Orzeszko, F. Meggio, Z. Kazimierczuk and L. A. Pinna, *Bioorg. Med. Chem.*, 2009, **17**, 7281–7289.
22 A. Gratz, U. Kuckländer, R. Bollig, C. Götz and J. Jose, *Mol. Cell. Biochem.*, 2011, **356**, 83–90.
23 P. Zień, M. Bretner, K. Zastapiło, R. Szyszka and D. Shugar, *Biochem. Biophys. Res. Commun.*, 2003, **306**, 129–133.
24 J. L. Stebbins, S. K. De, P. Pavlickova, V. Chen, T. Machleidt, L. H. Chen, C. Kuntzen, S. Kitada, M. Karin and M. Pellecchia, *J. Med. Chem.*, 2011, **54**, 6206–6214.
25 R. Battistutta, M. Mazzorana, S. Sarno, Z. Kazimierczuk, G. Zanotti and L. A. Pinna, *Chem. Biol.*, 2005, **12**, 1211–1219.
26 S. Sarno, E. Papinutto, C. Franchin, J. Bain, M. Elliott, F. Meggio, Z. Kazimierczuk, A. Orzeszko, G. Zanotti, R. Battistutta and L. A. Pinna, *Curr. Top. Med. Chem.*, 2011, **11**, 1340–1351.
27 K. Niefind, C. W. Yde, I. Ermakova and O. G. Issinger, *J. Mol. Biol.*, 2007, **370**, 427–438.
28 M. A. Pagano, J. Bain, Z. Kazimierczuk, S. Sarno, M. Ruzzene, G. Di Maira, M. Elliott, A. Orzeszko, G. Cozza, F. Meggio and L. A. Pinna, *Biochem. J.*, 2008, **415**, 353–365.
29 R. Battistutta, G. Cozza, F. Pierre, E. Papinutto, G. Lolli, S. Sarno, S. E. O'Brien, A. Siddiqui-Jain, M. Haddach, K. Anderes, D. M. Ryckman, F. Meggio and L. A. Pinna, *Biochemistry*, 2011, **50**, 8478–8488.

30 P. P. Graczyk, *J. Med. Chem.*, 2007, **50**, 5773–5779.
31 A. Vaasa, M. Lust, A. Terrin, A. Uri and M. Zaccolo, *Biochem. Biophys. Res. Commun.*, 2010, **397**, 750–755.
32 C. S. Chen and M. Poenie, *J. Biol. Chem.*, 1993, **268**, 15812–15822.
33 A. Vaasa, I. Viil, E. Enkvist, K. Viht, G. Raidaru, D. Lavogina and A. Uri, *Anal. Biochem.*, 2009, **385**, 85–93.
34 D. Shugar, *Acta Biochim. Pol.*, 1996, **43**, 9–23.
35 N. Grankowski, B. Boldyreff and O. G. Issinger, *Eur. J. Biochem.*, 1991, **198**, 25–30.
36 I. Ermakova, B. Boldyreff, O. G. Issinger and K. Niefind, *J. Mol. Biol.*, 2003, **330**, 925–934.
37 R. A. Copeland, *Evaluation of Enzyme Inhibitors in Drug Discovery: A Guide for Medicinal Chemists and Pharmacologists*, ed. R. A. Copeland, John Wiley & Sons, Inc., 2005, pp. 178–213.
38 W. Kabsch, *Acta Crystallogr., Sect. D: Biol. Crystallogr.*, 2010, **66**, 125–132.
39 M. D. Winn, C. C. Ballard, K. D. Cowtan, E. J. Dodson, P. Emsley, P. R. Evans, R. M. Keegan, E. B. Krissinel, A. G. Leslie, A. McCoy, S. J. McNicholas, G. N. Murshudov, N. S. Pannu, E. A. Potterton, H. R. Powell, R. J. Read, A. Vagin and K. S. Wilson, *Acta Crystallogr., Sect. D: Biol. Crystallogr.*, 2011, **67**, 235–242.
40 P. D. Adams, P. V. Afonine, G. Bunkoczi, V. B. Chen, I. W. Davis, N. Echols, J. J. Headd, L. W. Hung, G. J. Kapral, R. W. Grosse-Kunstleve, A. J. McCoy, N. W. Moriarty, R. Oeffner, R. J. Read, D. C. Richardson, J. S. Richardson, T. C. Terwilliger and P. H. Zwart, *Acta Crystallogr., Sect. D: Biol. Crystallogr.*, 2010, **66**, 213–221.
41 P. Emsley, B. Lohkamp, W. G. Scott and K. Cowtan, *Acta Crystallogr., Sect. D: Biol. Crystallogr.*, 2010, **66**, 486–501.